

6. HIGHLIGHTS OF LABORATORY FOR ATMOSPHERES ACTIVITIES IN 1997

Scientists in the Laboratory for Atmospheres have contributed directly to the advancement of Earth and space science by publishing 176 articles in refereed journals during the past year; a list of these publications is found in [Section 14](#). Laboratory scientists have also presented talks and written articles for public and professional audiences. Other publications by Laboratory scientists include NASA Technical Memoranda, technical books and book chapters, and position papers related to national and international scientific policy issues.

In this section we present a few examples selected from work completed or nearly completed during 1997. The selection process was somewhat subjective; only time will tell the ultimate impact that these contributions will have.

All the highlights listed below are the achievements not only of civil servants and non-government personnel who work in the Laboratory, but also of many other colleagues at GSFC, at NASA Headquarters, at other NASA centers, most notably Ames Research Center, Langley Research Center, the Jet Propulsion Laboratory, and Marshall Space Flight Center. Private companies, other government laboratories, and universities in the United States and abroad have all made significant contributions to the work done in the Laboratory.

Ozone and Trace Gas Studies

Role of Pollutants in Ozone Formation in the Tropical Troposphere

Analysis of trace gas measurements taken by instruments on DC-8 aircraft during flights over Brasilia, Brazil, in September 1992 confirms that thunderstorms inject pollutants into the upper troposphere, contributing to ozone formation in that part of the atmosphere where ozone is an effective greenhouse gas. The pollutants (carbon monoxide and nitrogen oxides) come from biomass burning and were measured near savannah fires by the DC-8. The pollutants also are carried upward in the storm cell and stream out of the anvil, traveling toward the Atlantic, making more ozone along the way. Lightning also created NO and made a contribution to upper tropospheric ozone formation. A chemical box model was used to calculate the amount of ozone formed en route over the Atlantic. These calculations showed levels of ozone at 20-30 ppbv at 9-12 km; this increase was actually observed with ozone sensors on balloons at an Atlantic coast site two to three days downwind.

Thompson, A.M., W.-K. Tao, K. E. Pickering, J. R. Scala, and J. Simpson, Tropical Deep Convection and Ozone Formation, *Bull. Amer. Met. Soc.*, 78, 1043-1054, 1997.

Long Term Changes in Tropospheric Column Ozone in the Tropics

A new technique for deriving tropospheric column ozone was developed by Laboratory staff. This technique, the connective-cloud differential (CCD) technique, enables characterization of the spatial and temporal changes in tropospheric column ozone in the tropics derived from the Total Ozone Mapping Spectrometer (TOMS) high-density footprint measurements. The technique is based on the fact the TOMS instrument measures column ozone only above cloud heights. In the tropics, the high reflecting convective clouds extend up to the tropopause and persist over an extended region. This allows one to derive tropospheric column ozone by simply measuring the stratospheric column ozone above cloud levels and subtracting it from the total column ozone measured from the nearby cloud free regions. By combining high-density total ozone and reflectivity footprint TOMS data obtained during the lifetime of the Nimbus-7 satellite (November 1978-May 1993), the Earth Probe (July 1996-present), and the Japanese Advanced Earth Observing Satellite (September 1996-June 1997), we have derived long time series of tropospheric column ozone, particularly in the regions of high convective clouds. These time series provide important insight regarding the seasonal, interannual, and decadal variabilities in tropospheric column ozone.

Our study suggests that most of the increase in the tropospheric ozone observed in the tropical Atlantic region is a manifestation of transport associated with the convergent-divergent east-west Walker circulation, and is not necessarily caused by ozone precursors (e.g., CO, NO_x and hydrocarbons) produced in biomass burning, as generally believed. The changes in this circulation pattern causes an interannual variability in tropospheric ozone which is correlated with the changes in sea surface temperature as inferred from the Southern Oscillation Index (SOI). This is quite distinct from the interannual variability in stratospheric column ozone which is related to the quasi-biennial oscillation (QBO).

Chandra, S., J. R. Ziemke, and W. Min, The Origin of the Zonal Anomaly in Tropospheric Ozone: Dynamics And/or Biomass Burning, *Geophys. Res. Lett.*, 1997 (submitted)

Ziemke J. R., and S. Chandra, On Tropospheric Ozone and Tropical Wave 1 in Total Ozone, *Quad. Ozone Symp. Proc.*, 1997 (in press)

Ziemke, J. R., S. Chandra and P. K. Bhartia, Tropospheric Ozone Derived from the Combined UARS MLS/HALOE and High-Density TOMS Measurements, *J. Geophys. Res.* 1997 (Manuscript in preparation)

Low Ozone over the Arctic

Total ozone observations from the Total Ozone Mapping Spectrometer (TOMS) instruments during March 1997 reveal an extensive region of low ozone values in the Arctic region centered near the north pole. The observations show ozone values below 250 Dobson units (DU) for nearly a two-week period that are correlated with the position of the northern polar vortex. The March 1997 average ozone values are 40% lower than values observed during the same period in 1979-1982. This ozone low was highly correlated with the polar vortex, and exhibited rapid reductions in column amounts during the spring period as the sun rises over the Arctic. Values began to recover in late March and early April.

The rapid decline of total ozone over the Arctic during February and March 1997 is consistent with in-situ chemical loss. The large decrease of total ozone is contained within the lower stratospheric polar vortex, and is not directly impacted by vertical transport processes. Cold temperatures persisted into late March, most likely enhancing active chlorine via heterogeneous reactions on the surfaces of cold sulfate aerosols, and this reactive chlorine then catalytically destroyed ozone.

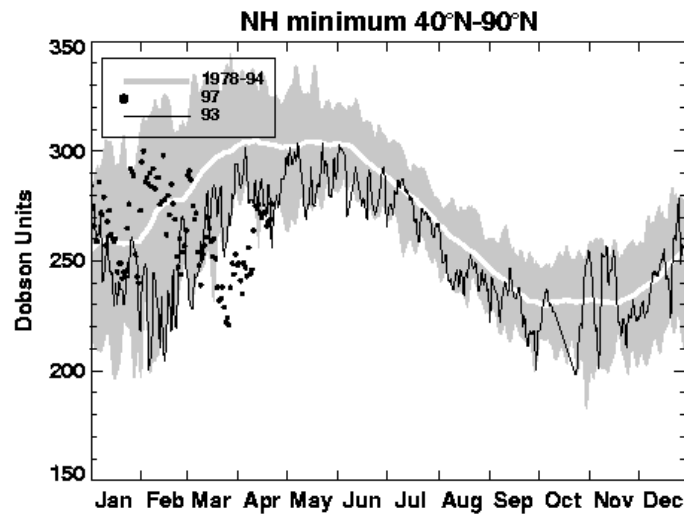


Figure 3. Daily minimum total ozone values observed between 40 and 90 degrees North during 1997 (dots), and 1993 (thick line). The range of minimum values for the years 1978 to 1994 is indicated by the gray shading, while the average minimum value is indicated by the thick white line. Record low values were measured in late March and early April in the polar region.

Coy, L., E.R. Nash, and P.A. Newman, Meteorology of the Polar Vortex: Spring 1997, *GRL*, 24, 2693-2696, 1997

Newman, P.A., J.F. Gleason, R.D. McPeters, and R.S. Stolarski, Anomalous Low Ozone Over the Arctic, *GRL*, 24, 2689-2692, 1997

Activation of Chlorine in Stratospheric Sulfate Aerosol

Recent research provides the strongest observational evidence to date that key reactions of chlorine species which lead to polar ozone depletion (e.g. the Antarctic ozone "hole") can occur on the surfaces of sulfate aerosol particles at cold temperatures. These particles are ubiquitous in the stratosphere. Previous conceptual models of ozone depletion required the formation of polar stratospheric clouds (PSC) to initiate the chlorine reactions.

Measurements were obtained from the NASA ER-2 stratospheric sampling aircraft during flights from Christchurch, New Zealand, toward Antarctica. The abundance of reactive chlorine in the lower stratosphere was observed to increase sharply with exposure to temperatures below about 195 K, a temperature which is near the nitric acid trihydrate (NAT) equilibrium condensation point. Back trajectories from the aircraft sampling points indicated that the sampled air was cooling at the rate of 20 to 30 K/day to temperatures below the NAT condensation point and had not been below the NAT condensation point prior to that for at least 10 days. Hence, the observed amount of active chlorine should be kinetically limited by the recent parcel temperatures. The measurements showed enhanced ClO and decreased HCl at temperatures below 195 K, even in the absence of significant PSC particle surface area.

Kawa, S. R., P. A. Newman, L. R. Lait, M. R. Schoeberl, R. M. Stimpfle, D. W. Kohn, C. R. Webster, R. D. May, D. Baumgardner, J. E. Dye, J. C. Wilson, K. R. Chan, M. Loewenstein, Activation of Chlorine in Sulfate Aerosol as Inferred from Aircraft Observations, *J. Geophys. Res.*, 102, 3921-3933, 1997.

Modeling of Upper Atmospheric Research Satellite Data to Generate Ozone Forecasts

The three-dimensional chemistry and transport model, which uses winds and temperatures from the Goddard Earth Observing System Data Assimilation System (GEOS-DAS) has been applied to the analysis of a broad suite of observations from the Upper Atmosphere Research Satellite (UARS) to clarify the photochemical and transport processes both of which contribute to ozone evolution in the middle stratosphere. The model is being used in support of the POLARIS mission; a full chemistry integration is being carried out in near-real-time so that the three-dimensional modeled fields may provide a context for aircraft observations. The model is also being used with simplified photochemistry to provide five-day forecasts of the ozone field to assist in flight planning.

Douglass, A.R., R. B. Rood, S. R. Kawa and D. J. Allen, A Three-dimensional Simulation of the Evolution of the Middle Latitude Winter Ozone in the Middle Stratosphere, *J. Geophys. Res.*, 102, 19,217-19,232, 1997.

Validation of Langley Airborne Lidar during TOTE/VOTE

During the Tropical Ozone Transport Experiment (TOTE)/Vortex Ozone Transport Experiment (VOTE) mission in 1995/1996, the Stratospheric Ozone Lidar made ground-based measurements beneath the flight path of the DC-8 aircraft, which was carrying an airborne ozone lidar. The results of these simultaneous measurements showed that several errors existed in the algorithm used to extract ozone data from the airborne lidar.

Grant, W.B., M.A. Fenn, E.V. Browell, T.J. McGee, U.N. Singh, M.R. Gross, I.S. McDermid, P.-H. Wang, L.E. Deaver, and L. Froidevaux, Correlative Stratospheric Ozone Measurements with the Airborne UV DIAL System during TOTE/VOTE, Submitted to *Geophys. Res. Lett.*, June, 1997

Satellite Estimation of Surface Ultraviolet Flux

A technique developed previously for estimating surface ultraviolet (UV) flux from satellite data has been refined by incorporating the effects of snow/ice reflection and providing a better correction for attenuation of the signal by clouds.

Detailed comparisons with ground-based instruments have verified model calculations that show that the total ozone in the Earth's atmosphere almost exclusively determines the ratio of biologically damaging UV-B radiation and (relatively) benign UV-A radiation. Clouds and aerosols affect both UV-A and UV-B radiation about equally, and thus do not affect the ratio.

This important finding allows the UV-B/UV-A ratio to be estimated with a precision of 1%/decade over the entire globe using the 17-year data record of Total Ozone Mapping Spectrometer (TOMS) series of instruments. TOMS data also show that both UV-A and UV-B radiation can be greatly reduced by the presence of wind-blown dust from the

deserts, and smoke from agricultural biomass burning. These effects, primarily confined to the tropics, are potentially as biologically important as an increase in UV due to ozone depletion, which primarily affects mid- and high latitudes. The relative importance of these effects is currently under active investigation.

Herman, J.R., P.K. Bhartia, J. Ziemke, Z. Ahmad, D. Larko, UV-B Increases (1979-1992) From Decreases In Total Ozone, *Geophys. Res. Lett.* 23(16) 2117-2120, 1996

Remote Sensing of Clouds and Water Vapor

Scanning Raman Lidar Measurements of Clouds, Water Vapor, and Aerosols

During a recent field campaign at Wallops Island, Virginia, the NASA/GSFC Scanning Raman Lidar (SRL) measured, in the water vapor channel, Raman scattering from low-level clouds well in excess of 100% relative humidity. This excess scattering has been interpreted to be spontaneous Raman scattering by liquid water in the cloud droplets, and indicates that this phenomenon may provide a remote method to observe cloud liquid water.

Data acquired by the SRL during the Tropospheric Aerosol Radiative Forcing Observational Experiment (TARFOX) have also been used to derive aerosol extinction and aerosol optical thickness as a function of altitude and time. Vertical profiles of aerosol optical properties are required to determine the surface and atmospheric radiation budget and the radiative forcing from anthropogenic aerosols. The lidar measurements are important since these profiles cannot be derived from surface aerosol measurements alone. The lidar profiles of aerosol backscattering and extinction are used to compute aerosol radiative effects throughout the entire atmospheric column and to assess the contributions of different aerosol layers to the column integrated measurements acquired by surface and satellite based sensors.

During the First Water Vapor Intensive Operations Period (IOP), which was held at the Department of Energy Atmospheric Radiation Measurement (ARM) Southern Great Plains (SGP) site in September 1996, the SRL measured water vapor during both daytime and nighttime operations in order to help characterize the water vapor in the lowest kilometer of the atmosphere, and to develop an accurate calibration of the SGP Raman lidar without relying on radiosondes. Since previous water vapor comparisons at this site revealed uncertainties in water vapor measurements too large to assess the performance of radiation models at the level required for climate studies, the lidar water vapor measurements are used to investigate these uncertainties. Figure 4 shows an example of how the SRL data are used in profile comparisons, point measurements, and integrated precipitable water amounts. The SRL data showed that the water vapor measurements acquired during this IOP generally agree within about 5% which approaches the level required for climate studies.

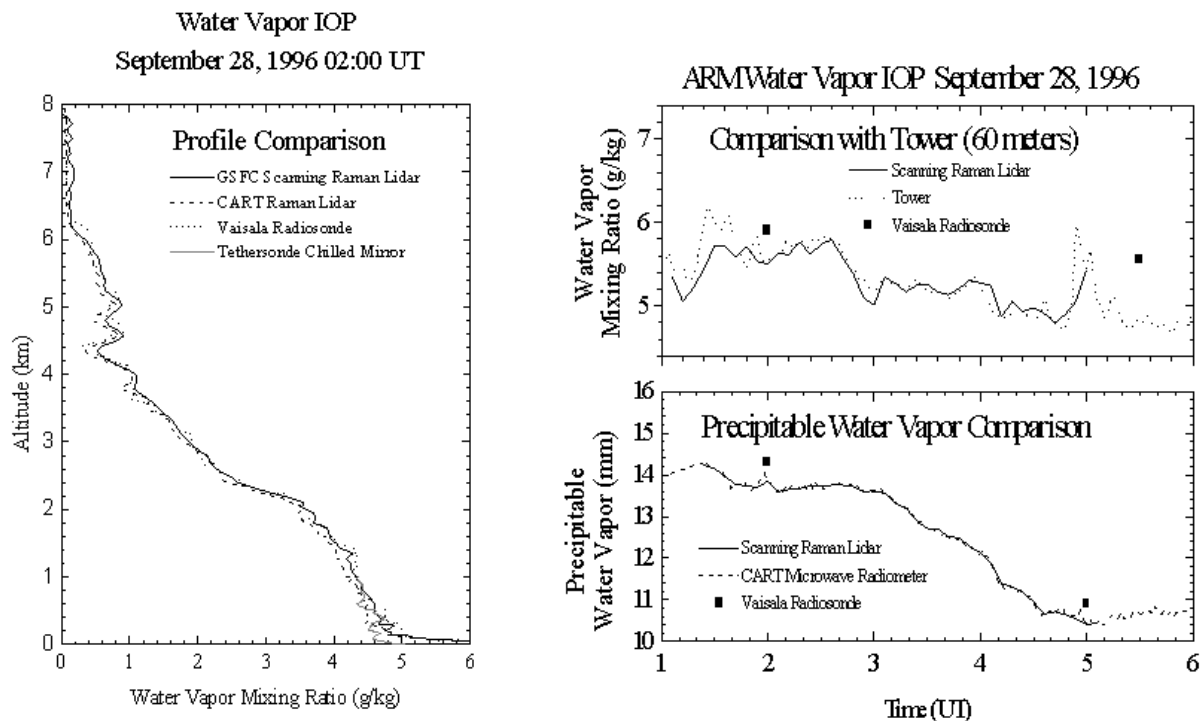


Figure 4. SRL water vapor comparisons using data acquired on the night of September 28, 1996 during the First Water Vapor Intensive Operations Period held at the Southern Great Plains site.

In the near future, SRL water vapor measurements will be used to both verify and assess aircraft and satellite based water vapor measurements and, depending upon the proximity to convective storms, provide detailed, nearly continuous mapping of the water vapor in the vicinity of convective storms.

Melfi, S.H., K.D. Evans, J. Li, D. Whiteman, R. Ferrare, G. Schwemmer, Observation of Raman Scattering by Cloud Droplets in the Atmosphere, *Appl. Optics*, 36(15), 3551-3559, 1997.

Rainfall Studies

Sampling Error in Satellite Estimates of Monthly Average Rainfall

Satellite data are used to produce gridded maps of monthly rainfall, but these averages are subject to sampling error because satellites in low-Earth orbits (which produce the most accurate rain estimates) cannot view a region continuously. These error estimates are almost as important as the data themselves if climate researchers are to use the data quantitatively. Studies at various ground-based sites have been used to obtain estimates of what the sampling error would be at those sites, but these results need to be generalized to provide error estimates at all grid boxes.

A model has been developed for the error. It requires only knowledge of the pattern of observations of the grid box by the satellite and the average rainfall occurring there; both are easy to obtain. The model has been used to consolidate sampling error estimates from a number of ground-based sites around the world, and will aid users of satellite-derived rainfall maps to attach confidence levels to each grid value. This technique has also suggested a new method of analyzing the statistics of satellite estimates, uncovering sources of error different from sampling error. These errors are due to biases in the satellite estimates that vary for different types of rain. Errors such as these may not average to zero even during a period as long as a month.

Bell, T.L., P.K. Kundu, and C.D. Kummerow, Sampling Errors for Gridded Rainfall Averages Obtained from Low-Earth-Orbiting Satellites, *Proc. 13th AMS Conf. on Hydrology*, 9-12, Long Beach, CA, 1997.

A Precipitation Data Set from TOGA-COARE

The TRMM Office has produced a high-resolution, open-ocean rainfall dataset for use in validation of satellite rainfall estimates and in studies of tropical air-sea interactions involving mesoscale precipitation.

Derived from ship-borne radar observations during the Tropical Ocean Global Atmosphere- Coupled Ocean Atmosphere Response Experiment (TOGA-COARE) Intensive Observing Period, the dataset covers an area of approximately 120,000 km² near 2 S, 156 E for the interval from November 5, 1992 to February 23, 1993. The rainfall rate product, with a spatial resolution of 4 km², every 10-minutes, has been used in the 3rd Algorithm Intercomparison Project (AIP-3) of the Global Precipitation Climatology Project (GPCP), and is available to the public on the Internet. The database includes information on the vertical structure of radar reflectivity within precipitating cloud systems to help researchers refine and improve both satellite and ground validation algorithms for the flight phase of TRMM. Lagrangian subsets of the data base have been extracted over TOGA-COARE oceanographic research vessels for ongoing studies of the role of tropical precipitation in modifying the ocean salinity profile.

Ebert, E. E., M.J. Manton, P.A. Arkin, R.J. Allam, G.E. Holpin, and A. Gruber, Results from the GPCP Algorithm Intercomparison Programme, *Bull. Amer. Meteor. Soc.*, 77, 2875-2887, 1997.

Short, D.A., P.A. Kucera, B.S. Ferrier, J.C. Gerlach, S.A. Rutledge, O.W. Thiele, Shipboard Radar Rainfall Fields Within the TOGA-COARE IFA. *Bull. Amer. Meteor. Soc.*, accepted August 21, 1997, to appear in December 1997.

Aerosol Studies

Dust Forcing of Climate Inferred from Correlations between Dust Data and Model Errors

Aerosol particles may affect climate through absorption and scattering of solar radiation; large dust particles may interact with thermal radiation, as well. There is some question as to whether atmospheric temperatures respond significantly to this type of radiative forcing, since feedback mechanisms can increase the effect or decrease it down to zero. So far, the temperature response has not been detected.

An indirect measure of the tropospheric temperature response has been developed using observationally-based increments from the NASA GEOS-1 DAS. These increments, which provide information about physical processes not included in the predictive model, have monthly mean patterns that bear a striking similarity to patterns of dust over the Atlantic Ocean. This similarity, and the high correlations between latitudinal location of maximum heating in atmospheric modeling updates and that of the number of dusty days, suggest that dust aerosols are an important source of errors in numerical weather prediction models over the Atlantic.

The jittered scatter plot shown in Fig. 5 shows a linear correlation coefficient between dust pixels and GEOS-1 DAS incremental analysis update (IAU) pixels of 0.41 increasing to 0.48 when zero-dust pixels are omitted. This work shows for the first time the response of the temperature field to the radiative forcing of the dust layer, although indirectly. The resulting heating rate of 6 K/year within the dust layer at 1.5-3 km is in agreement with calculated heating rates.

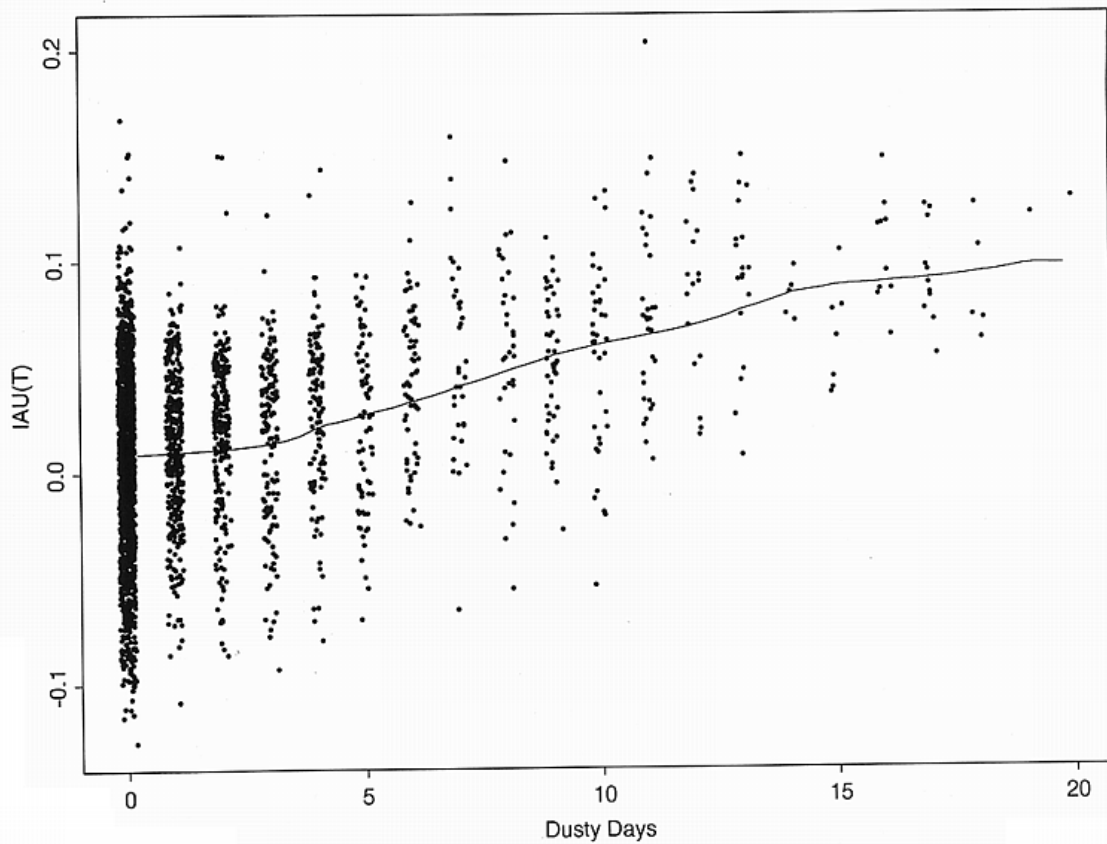


Figure 5. Jittered scatter plot for IAU(T) versus number of dusty days for each pixel: 208 points for each month - total of 2496 points. A moving locally weighted regression line is plotted and shows the saturation at a high number of dusty days.

Alpert, P., Y. Kaufman, Y. Shay-El, D. Tanre, A. daSilva, S. Schubert, and J. H. Joseph, Dust Forcing of Climate Inferred from Correlations Between Dust Data and Model Errors. Accepted for publication in *Nature*, 1997

Measurements of Winds

Tropospheric Wind Profiling Demonstrated with Direct Detection Doppler Radar

Lidar measurements of wind profiles in the troposphere have been using the edge technique Doppler lidar system. This follows the successful validation campaign in which the lidar was used to obtain high-precision (0.1 m/s), high-vertical-resolution (22 m) profiles of winds to altitudes of up to 2 km. The Laboratory-based lidar system was redesigned to extend the operating range into the troposphere. The principle improvement came from implementing the double edge technique, which has higher sensitivity than other techniques, and allows operation in regions of the atmosphere where the aerosol concentration is low.

Double Edge Lidar Wind Profiles

June 27, 1997

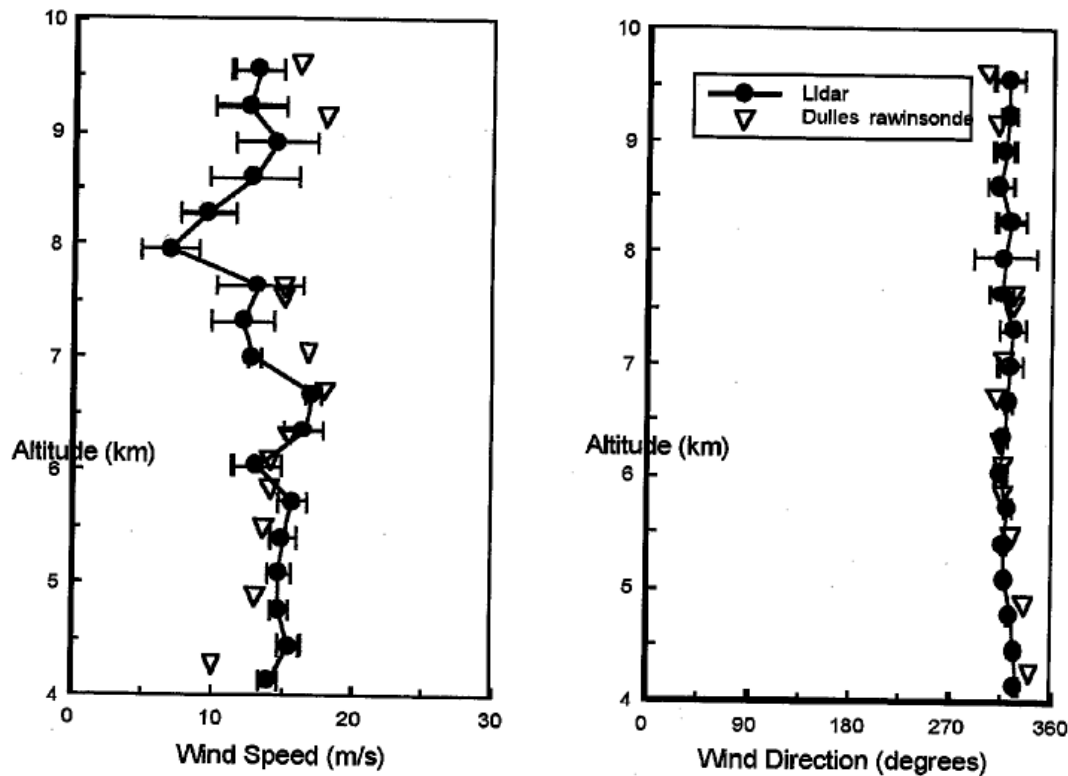


Figure 6. Lidar profiles of tropospheric wind speed and direction obtained with the ground-based "Double-Edge" Doppler Lidar. The mean and standard deviation of five independent lidar profiles are shown as a function of altitude. Upper air wind soundings obtained from the National Weather Service station at Dulles Airport are also shown for comparison.

The first tropospheric wind profiles were obtained from our laboratory in June, 1997. Wind speed and direction have been measured to altitudes of 12 km using the new system with a vertical resolution of 330 m. The lidar wind measurements have been compared with upper air soundings from Dulles airport; agreement between the two data sets is good.

This demonstration of tropospheric wind measurement capability is a key milestone in developing this technique as a candidate for future satellite wind-sensing missions. The measurements can also be used to verify instrument models used to design future space systems; this approach can also fulfill a critical need for direct measurement of tropospheric winds from satellites.

The laboratory lidar system is a prototype design which has been repackaged and will be mounted in a van early in 1998 so that field measurements of winds can be obtained in a variety of locations and atmospheric conditions. The van also serves as a mobile testbed to validate new technologies to be used in future space missions. This program is part of NASA's New Millennium Program.

Korb, C.L., B. Gentry, S.X. Li, Edge Technique Doppler Lidar Wind Measurements With High Vertical Resolution, *Applied Optics*, Aug. 20, 1996.

Korb, C.L., B. Gentry, S.X. Li, C. Flesia, Theory of the Double Edge Technique Doppler lidar wind measurement (submitted for publication in *Applied Optics*, Feb, 1997).

Middle Atmosphere Studies

Equatorial Oscillations in the Middle Atmosphere Generated by Gravity Waves

For almost three decades, based on the seminal work of Lindzen and Holton, it has been understood that the circulation of the middle atmosphere is to a large extent driven by upward propagating waves. The relative importance of small-scale gravity waves (GW) and planetary waves (PW), however, is only now beginning to emerge, in part through the development of advanced models.

Global scale models cannot resolve GW, and parameterization is needed to describe their effects. The Doppler Spread Parameterization (DSP) of Hines for the momentum deposition of GW is more realistic than other formulations in that it deals with a spectrum of waves and it accounts for the interactions between the waves and the background wind field and between the waves themselves; it also provides a description of the eddy viscosity. The DSP has now been incorporated into the 2D version of a non-linear, numerical spectral model (NSM) of the atmosphere, originally developed for solar and planetary applications. This model correctly reproduces the anomalous reversal in the seasonal temperature variations of the upper mesosphere, as did other models. More significantly, the model generates relatively large oscillations in the zonal circulation at low latitudes.

At 50 km, the computed amplitude of the Semi-Annual Oscillation (SAO) approaches 20 m/s, close to the observed values of 20-30 m/s. Higher up, near 85 km, the computed SAO reveals a secondary maximum, exceeding 10 m/s (20-30 m/s observed). This oscillation is in opposite phase to that near 50 km, in agreement with observations. In the stratosphere, the computed variations in the zonal wind exhibit a periodicity of more than 20 months, approaching the lower end of the observed Quasi Biennial Oscillation

(QBO); the computed winds reach almost 10 m/s, about half of those observed. The QBO, which was thought to be confined to altitudes below 50 km, is seen in the model extending up to 90 km; this has been confirmed by UARS measurements.

These results are significant in light of recent simulations with the Princeton General Circulation Model that resolves PW but not GW; this model produces a very weak QBO, an order of magnitude smaller than observed.

Mayr, H.G., J. G. Mengel, C. O. Hines, K. L. Chan, N. F. Arnold, C. A. Reddy, H. S. Porter, The Gravity Wave Doppler Spread Theory Applied In A Numerical Model Of The Middle Atmosphere: 2. Equatorial Oscillations, *J. Geophys. Res.*, in press, 1997

Atmospheric Variability and Predictability

Multiscale Processes in the Tropical Pacific Warm Pool

The analysis of TOGA-COARE data and related modeling studies have yielded new insights into the mechanism of multiscale organization of tropical intraseasonal variability in the tropical western Pacific warm pool (WPWP) region. Results show that a seesaw in anomalous convection and large-scale vertical motion between the Indian ocean and the western Pacific was responsible for the cycles of dry-wet phases in the WPWP. During the wet phase, subsynoptic scale atmospheric disturbances with quasi-periodicity of two to three days and diurnal variations in the atmosphere were very pronounced. During the dry phase, diurnal cycles in sea surface temperature (SST) was much enhanced, while the ocean mixed layer was much shallower than in the wet phase. Atmospheric diurnal variations over the equatorial warm ocean were dominated by nocturnal convection/rainfall in the disturbed periods when more moisture supply is available. During the undisturbed periods, the diurnal cycle in SST produced a mid-day maximum, which through boundary layer heating resulted in the occurrence of strong afternoon showers. Afternoon rainfall comes mostly from convective cells, but the nocturnal rainfall is derived from deeper convective cells and large areas of stratiform clouds.

Results of experiments with a two-dimensional version of the Goddard Cumulus Ensemble (GCE) model coupled to an ocean mixed layer model, suggested that the nocturnal rainfall maximum is associated with more available precipitable water at night (and less during the day) due to the diurnal radiative cooling/heating cycle. Based on numerical studies carried out to examine the penetrative absorption of solar radiation in the upper ocean and its effect on the ocean mixing processes, we concluded that the diurnal mixing cycle and the associated asymmetric heating cycle play a crucial important role in maintaining the intraseasonal variations in the upper ocean. Such intraseasonal variations play an important role in determining the characteristics--and often govern the timing--of the occurrences of El Nino.

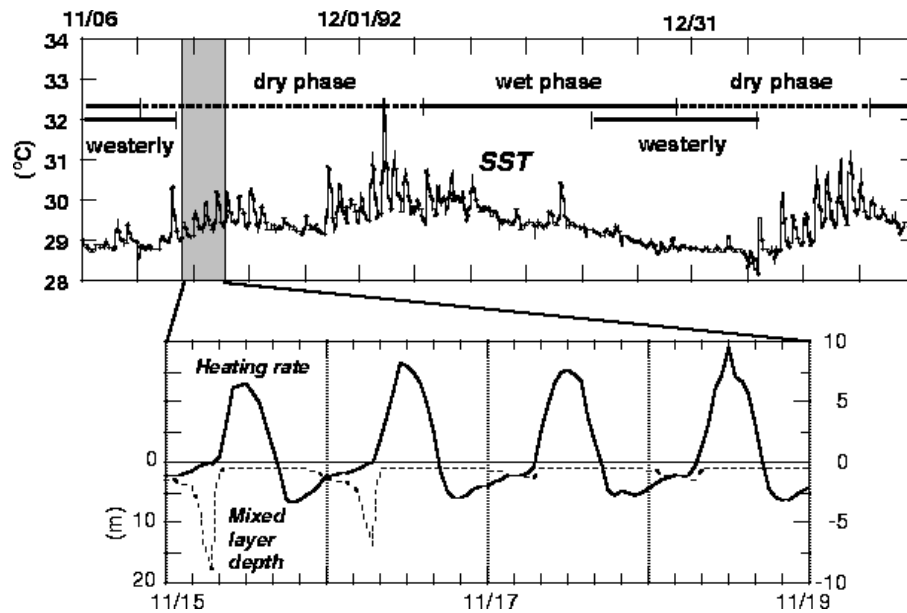


Figure 7. Top: Sea-surface Temperature in the tropical warm pool shows distinct intraseasonal and diurnal variations. **Lower:** Asymmetric heating and mixed layer depth, largely controlled by absorbed solar radiation near the surface.

These results indicate that detailed air-sea interaction processes--including those associated with the diurnal cycles--have to be incorporated into coupled ocean-atmosphere models to better simulate the air-sea fluxes and upper ocean feedback to changes in atmospheric forcings for seasonal-to-interannual scale variabilities.

Sui, C.-H., X. Li, K.-M. Lau, and D. Adamec, Multi-scale Air-sea Interactions During TOGA- COARE, *Mon. Wea. Rev.* 125, 448-462, 1997.

Sui, C.-H., K.-M. Lau, Y. Takayabu, and D. Short, Diurnal Variations in Tropical Oceanic Cumulus Ensemble During TOGA- COARE, *J. Atmos. Sci.* 54, 639-655, 1997.

Sui, C.-H., X. Li, and K.-M. Lau, Radiative-convective Processes in Simulated Diurnal Variations of Tropical Oceanic Convection, *J. Atmos. Sci.* (conditionally accepted, 1997)

Sui, C.-H., X. Li, and K.-M. Lau, Selective Absorption of Solar Radiation and Upper Ocean Temperature in the Equatorial Western Pacific, *J. Geophys. Res.* (in revision, 1997)

New Understanding of Asian Monsoon Predictability

The Asian monsoon affects over 60% of the world's population, and is one of the most important source/sink regions for the global hydrologic cycle. For centuries, it has been known that SST and ground wetness (GW, including soil moisture and snow cover) have strong impacts on the seasonal-to-interannual predictability of the Asian monsoon. Yet, because of the interactive nature of SST and continental scale GW it has been difficult, if not impossible, to separate the causal factors among SST, GW and the Asian monsoon. Using assimilated data from the DAO, satellite-derived rainfall, and numerical model experiments, scientists at the Climate and Radiation Branch have documented regional features--and unraveled some of the mysteries surrounding the age-old predictability problem--of the Asian monsoon.

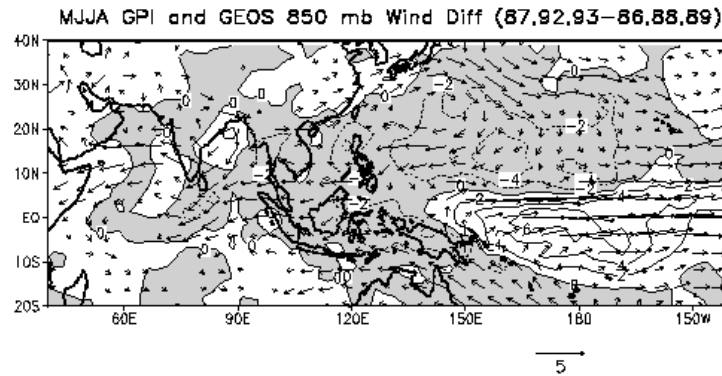


Figure 8. Relationship between ENSO and Asian Monsoon for Northern Summer (May - August) showing composite differences between rainfall (contours in mm/day) and 850 mb winds (vectors in m/s) between warm and cold events. The rainfall is from the Global Precipitation Climatology Project (GPCP); the winds are derived from the NASA GEOS analysis.

Results indicate that basin-scale SST anomalies associated with the El Niño-Southern Oscillation (ENSO) exert a stronger control on the interannual variability of the broad scale monsoon than do corresponding GW anomalies. A warm event (El Niño) is associated with a weakened Asian monsoon (and vice versa for a cold event) through establishment of an anomalous Walker circulation with anomalous subsidence over the monsoon region. However, in terms of the magnitude and the spatial distribution of the anomaly patterns of rainfall and SST, the impact of SST anomalies on the Asian monsoon is quite nonlinear with respect to the warm and the cold events; the warm events generally have a much wider impact compared to the cold events.

We also found that following a wet and cold spring over the continent, the Asian monsoon is generally weaker than under other conditions; the wet and cold conditions may be caused by an El Niño. The results suggest that land surface processes may interact with atmospheric anomalies induced by SST anomalies, amplifying the anomalies. When realistic SST and GW forcings are introduced separately, the magnitude of precipitation anomalies caused by SST relative to GW is about 5 to 1. This implies that, for long-term prediction of the Asian monsoon, better monitoring of the Pacific Ocean by satellite or from buoys is of the highest priority. Monitoring snow cover and soil moisture over Eurasia will also significantly improve the prediction of the Asian monsoon.

Lau, K-M, and W. Bua, Internal Dynamics, SST, Soil Moisture and the Asian Monsoon: Insights from GCM Experiments. *J. Climate* (submitted, 1997).

Yang, S. and Lau, K-M., Influence of Sea Surface Temperature and Ground Wetness on the Asian Summer Monsoon, *J. Climate* (conditionally accepted, 1997).

Lau, K.-M, and S. Yang, Climatology and Interannual Variability of the Southeast Asian Monsoon, *Adv. Atmos. Sci.*, 14, 141-162, 1997.

Satellite Sensing of Global Warming

The Microwave Sounding Unit (MSU) is a passive microwave radiometer flown on the NOAA operation satellite series. Measurements made in channel 2 (53.74 GHz) of this instrument respond to the mid-tropospheric temperature, which is closely related to surface air temperature. Therefore, MSU has the potential to detect global temperature change.

Preliminary estimates of the global temperature from MSU made by Spencer and Christy in 1990 showed that global temperature stayed nearly the same in the period 1979-1988, while the analysis performed with conventional surface air temperature by Henson and Wilson in 1993 showed a warming of 0.2 K.

Recent studies by scientists at the Climate and Radiation Branch have shown that MSU temperature measurements were affected by contamination due to hydrometeors and systematic instrument calibration problems. Based on radiative transfer theory and MSU channel 2 measurements, we found that there were unscreened hydrometer contaminations present in the MSU data used by Spencer and Christy. This contamination can introduce an error in the MSU global temperature of about 0.05 K. We recently devised a methodology to correct for the calibration errors.

MSU Ch 2 Detected Global Warming

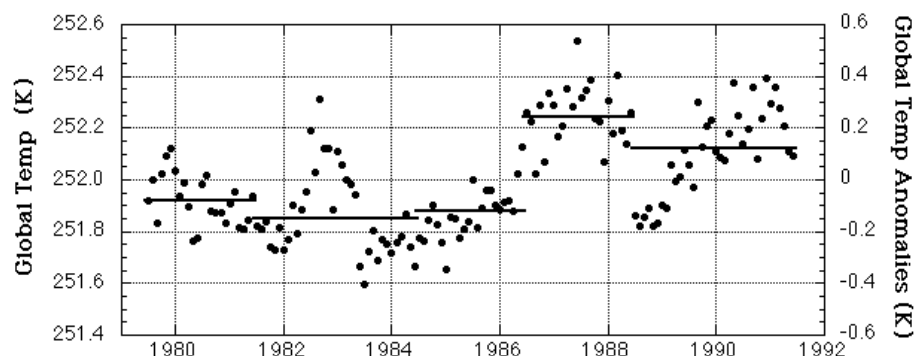


Figure 9. Corrected MSU Ch. 2 global temperature as a function of time. Solid lines correspond to the scale on the left ordinate, and represent global mean temperature deduced from successive satellites (NOAA 6, NOAA 7, NOAA 9, NOAA 10, and NOAA 11), covering the period from 1980-1991. The MSU observed warming from 1980 to 1991 is $0.23 \pm 0.12\text{K}$ (see text). Open circles correspond to the scale on the right ordinate, and denote monthly temperature anomalies with respect to the 12-year mean annual cycle.

Based on this research, we conclude that the estimation of global temperature based on satellite data can be used to monitor anthropogenic climatic effects, provided that proper procedures are carried out to remove contamination of the data by the presence of hydrometers and by instrument calibration errors.

Prabhakara, C., J.-M. Yoo, R. Iacovazzi, Jr., Global Warming Estimation from MSU, *J. Applied Meteorology* (submitted, 1997).

Air-Sea Surface Fluxes

Satellite Estimates of Air-Sea Turbulent Fluxes

Satellite algorithms have been developed to retrieve global air-sea turbulent fluxes (momentum, sensible heat, and latent heat) from Special Sensor Microwave/Imager (SSM/I) data, and then to study impacts of westerly wind bursts (WWB) on evaporation.

Daily mean air-sea turbulent fluxes retrieved during TOGA-COARE intensive observing period compare well with those obtained by a research vessel collocated in the western equatorial Pacific Ocean. Furthermore, global distributions and seasonal variability of monthly latent and sensible heat fluxes compare reasonably well with those derived from the conventional data-based Comprehensive Ocean Atmosphere Data Set (COADS).

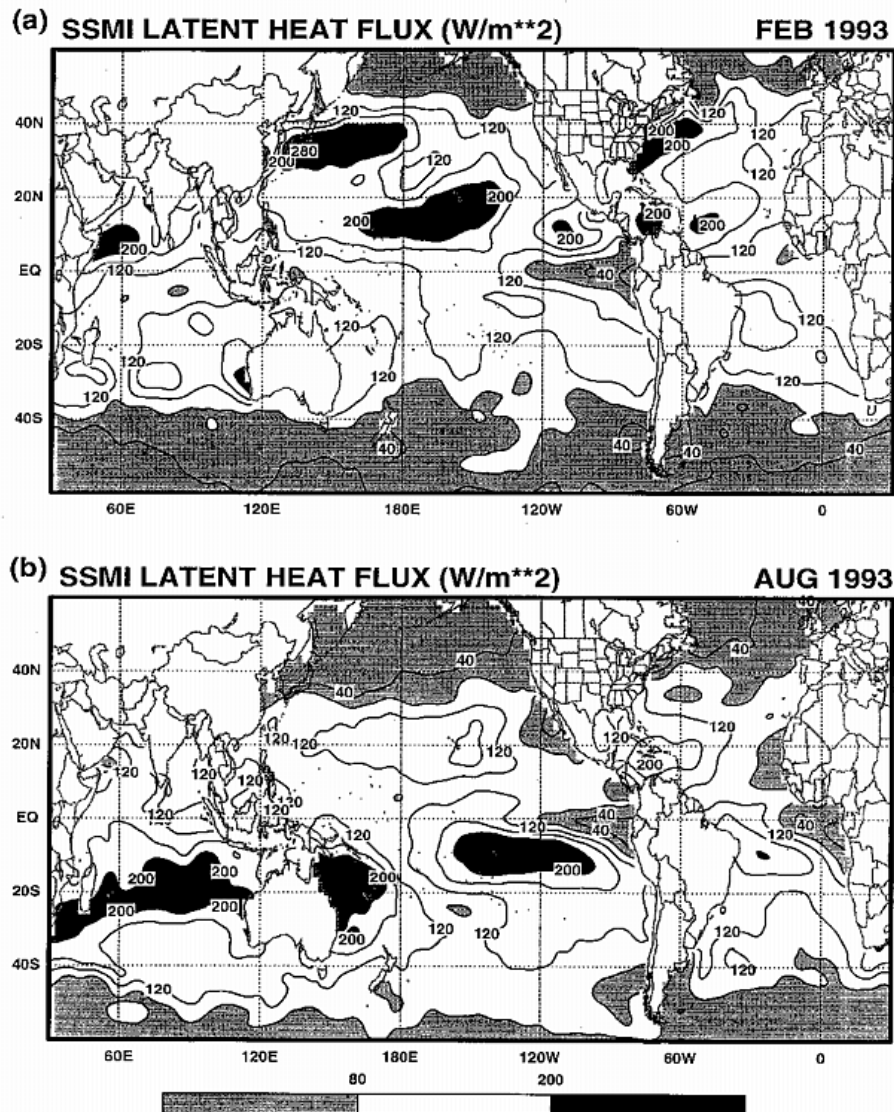


Figure 10. Monthly averages of daily SSM/I latent heat fluxes for (a) February and (b) August 1993. Daily flux is computed from daily SSM/I wind speed, Empirical Orthogonal Function (EOF) -retrieved SSM/I surface humidity, NCEP SST and ECMWF (SST-T(Air Temperature)) using the stability-dependent bulk scheme of Chou (1997).

The SSM/I derived sensible heat fluxes are generally within 10 Wm^{-2} of COADS. However, the satellite-based latent heat fluxes are generally larger (especially over the wintertime hemisphere) due mainly to the fact that the COADS underestimates wind speeds over the trade wind areas, and overestimates surface humidity. Further, errors arise from insufficient monthly measurements.

Global daily air-sea turbulent fluxes covering July 1987 to December 1994 have been produced using the algorithms. The results show that the patterns of latent (sensible) heat fluxes track well with those of sea-air humidity (temperature) differences. The maximum latent/sensible heat fluxes occur over the northwestern Pacific and Atlantic Oceans in February, where strong offshore winds carry the cold, dry continental air flowing over the warm Kuroshio Current and Gulf Stream. Large fluxes are also found for the latent heat flux in the trade wind zones of both hemispheres--with larger fluxes in the winter--due to a larger sea-air humidity difference coupled with stronger wind. Conversely, the sensible heat flux is very small over the tropical oceans and summertime extratropical oceans.

Based on our analysis, a WWB with a westerly surface zonal wind of 5-10 ms⁻¹ averaged over the 10-70S band develops in December 1992 over the equatorial Indian ocean, and propagates eastward to the equatorial central Pacific ocean from between November 1992 and January 1993. The WWB, with higher surface winds and drier air, and the associated super cloud cluster, which decreases solar heating, significantly increase the latent heat flux and decrease the sea surface temperature, with the maximum impact over the warm pool.

Chou, S.-H., C.-L. Shie, R. M. Atlas and J. Ardizzone, Air-sea Fluxes Retrieved from Special Sensor Microwave Imager Data. *J. Geophys. Res.*, 102, 12705-12726, 1997.

Data Assimilation Studies

Development of the GEOS-2 Assimilation System

The GEOS-2 assimilation system builds upon the baseline GEOS-1 DAS, which was used to produce the DAO 16-year (1980-95) reanalysis data set currently being used by numerous members of the research community. GEOS-2 is an intermediate, pre-launch system to be used for mission support, for short-term data experiments, and for participation in the Atmospheric Model Intercomparison and the Dynamical Seasonal Prediction Projects (AMIP II and DSP). It contains several major improvements over the GEOS-1 system, including improved radiation codes, enhanced vertical resolution and extent including a fully resolved stratosphere, a gravity-wave-drag parameterization, a numerical scheme which can reduce computational noise by rotating the pole, and a new Physical-Space Statistical Analysis System (PSAS).

GEOS-2 development involved several focused internal projects to integrate the new model and analysis systems and to provide a detailed evaluation of the new system. Many improvements were made, particularly in the parameterization of clouds and cloud-related fields, but much of this effort addressed two major system deficiencies: excessive noise in the stratospheric analysis and excessive warm-season continental rainfall. Horizontal and vertical error correlation functions have been modified, resulting in improved vorticity fields in the stratosphere that are both smoother and have a more realistic filamentary structure. Changes in the convective cloud parameterization and its interaction with the planetary boundary layer have resulted in modest improvements in the representation of warm-season continental rainfall, especially in the diurnal cycle of simulated precipitation over land surfaces. Further improvements in precipitation will require the development of a more accurate technique to vertically interpolate incremental updates of temperature and moisture from the analysis scheme onto the vertical grid of the prognostic model. This will be implemented as part of the first operational GEOS-3 DAS, scheduled to be completed in June of 1998.

Shubert, S.D., W. Min, L. Takacs, J. Joiner, Reanalysis of Historical Observations and its Role in the Development of the Goddard EOS Climate Data Assimilation System, *Adv. Space. Res.* 19(3), 491-501, 1997

Assimilation of Satellite Rainfall Retrieval

The DAO has developed a methodology for assimilating satellite-based precipitation data for improving global analysis for climate research. The results show that assimilation of the Goddard Profiling (GPROF) rainfall estimates in the tropics derived from the Special Sensor Microwave/Imager (SSM/I) instruments significantly improves the spatial and temporal distributions of clouds and latent heat release associated with convective activities in the tropics.

Assimilation of precipitation data in conjunction with SSM/I vertically integrated moisture data leads to reduced bias and root-mean-square error (up to 30%) in the outgoing longwave radiation at the top of the atmosphere, reflecting improvements in the overall quality of the assimilated data set. An improved cloud distribution can also improve the solar radiation estimates at the Earth's surface. These results suggest that assimilation of high-quality tropical rainfall data from the Tropical Rainfall Measuring Mission (TRMM) together with other available satellite rainfall and moisture data, can significantly improve the radiative and dynamic signals in global analyses. Accurate representations of tropical convection, clouds, and transport by the large-scale circulation in the global analysis are crucial to providing reliable diagnostics for investigating climate variability associated with events such as the El Nino and Southern Oscillation (ENSO), and understanding its impact on the global climate.

Hou, A.Y., D.V. Ledvina, A.M. da Silva, Assimilation of SSM/I Precipitation and Total Precipitable Water Retrievals for Improving Climate Signals in the GEOS Reanalysis, *Mon. Wea. Rev.*, (to be submitted, 1997).

A Three-Dimensional Ozone Assimilation System

A three-dimensional ozone assimilation system is being developed at the DAO. The initial aim is to provide high-quality, near-real-time, three-dimensional ozone fields as input to satellite instrument teams. In the longer term, we expect to use the data generated by the system also for process and trend studies. The assimilating model is the chemistry and transport model (CTM) developed jointly by the Atmospheric Chemistry and Dynamics Branch and the DAO at GSFC. The model is driven by GEOS-DAS assimilated wind fields; the input observations are TOMS total ozone and SBUV ozone profiles.

The analysis equations are solved in physical space; the system is being designed to work as a filter with continuous updates at every time step, rather than using a six-hourly forecast/analysis cycle as is common in assimilation for numerical weather prediction. The reason for this is that the ozone system is driven by satellite data obtained on a continuing basis, as opposed to meteorological systems that still rely extensively on conventional observations taken at the synoptic times. The method of continuous updates is computationally more efficient than the intermittent cycling, and it will also minimize phase errors due to the difference between the analysis time and the actual time of the observation.

Running the system in continuous update mode is made possible by the recent development at the DAO of a simple and inexpensive method for specifying forecast error correlations directly in terms of the forecast field itself. Standard meteorological analysis systems operate under the assumption that forecast error correlations, which, in turn, determine the physical shape of the analysis increments, are anisotropic. This is known generally not to be true, but the assumption has been used mainly for lack of affordable flow-dependent error models. The new model is easy to implement, and it has been shown to give significant improvement over an isotropic error model in a pilot study involving total ozone estimation.

Riishojgaard, L. P., A Direct Way of Specifying Flow-dependent Background Error Correlations for Meteorological Analysis Systems (accepted for publication in *Tellus*, 1997).

Evaluation of NASA Scatterometer Data and its Application to Weather Analysis and Forecasting

The NASA scatterometer (NSCAT) was launched on board the Japanese ADEOS satellite on August 16, 1996. Managed by the Jet Propulsion Laboratory (JPL), NSCAT provided an extensive data set of all weather wind observations over the global oceans until contact with ADEOS was lost in 1997.

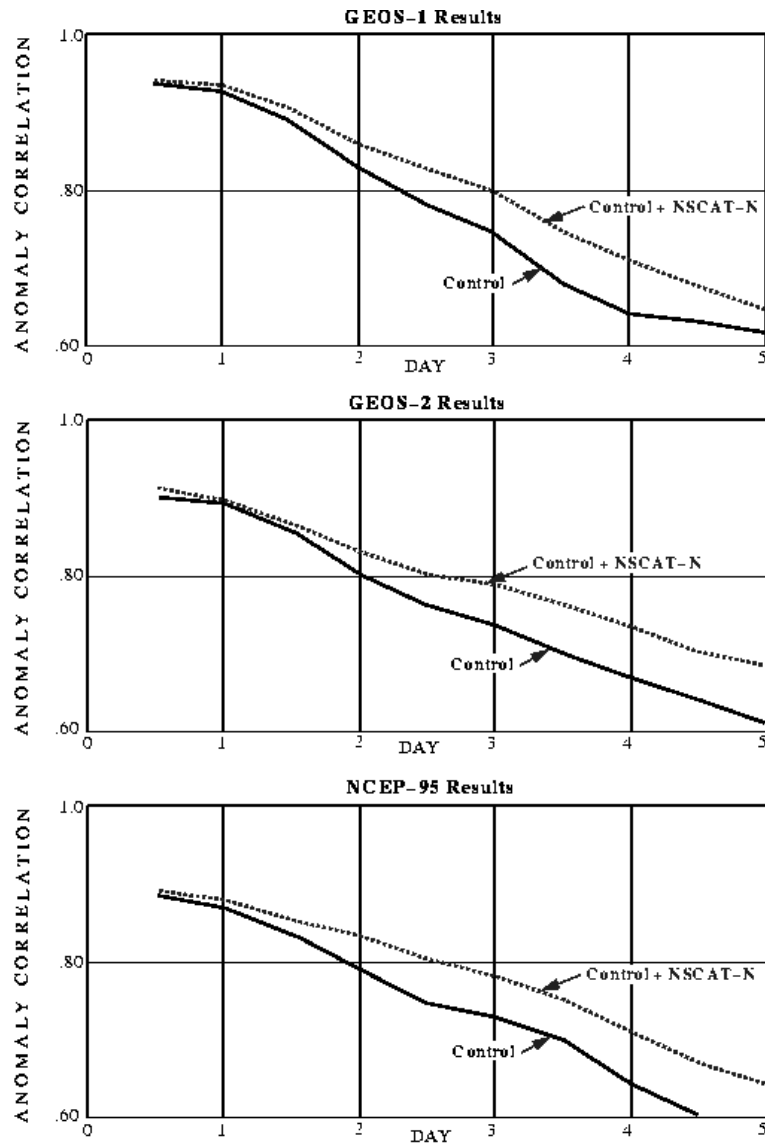


Figure 11. Impact of NSCAT wind vectors on Southern Hemisphere forecast of Sea Level Pressure using 3 different data assimilation systems. (Average of 8 five-day forecasts.)

A detailed geophysical evaluation of the initial NSCAT data sets was performed to determine the error characteristics of these data and their applicability to ocean surface analysis and weather prediction. The first component of this evaluation consisted of collocations of NSCAT data to ship and buoy wind reports, SSM/I wind observations, and National Center for Environmental Prediction (NCEP) and Goddard EOS (GEOS) model wind analyses. This was followed by data assimilation experiments to determine the impact of NSCAT data on analysis and forecasting.

Results from this evaluation indicated that NSCAT data is extraordinarily useful. The collocation comparisons showed the NSCAT wind velocity data to be of higher accuracy than European Remote Sensing (ERS-2) wind data. The impact experiments showed that NSCAT has the ability to correct major errors in analyses over the oceans and also to improve numerical weather prediction. NSCAT data typically show the precise locations of both synoptic-scale and smaller cyclones and fronts over the oceans. This often results in significant improvements to analyses. Forecast experiments using both the GEOS model and the NCEP model, which was operational in 1995, show approximately a one-day extension of useful forecast skill in the Southern Hemisphere. In the Northern Hemisphere the impact is smaller, but significant improvements in analyses and forecasts of storms occasionally occur.

Atlas, R., Preliminary Evaluation of NASA Scatterometer Data and Its Application to Ocean Surface Analysis and Numerical Weather Prediction, *Earth Observing Systems II, Society of Photo-Optical Instrumentation Engineers, Proceedings Reprint*, vol. 3117, 90-97, 1997.

Modeling Studies

Development of a Physically Consistent Finite-Volume General Circulation Model Based on the Conservative Flux-Form Semi-Lagrangian Transport Scheme

A physically consistent finite-volume "dynamical core" has been developed for the Goddard Earth Observing System General Circulation Model (GEOS GCM). Rather than the usual approach of modeling the dynamical processes in the atmosphere indirectly by discretizing the governing continuous differential equations, dynamical processes are modeled directly in the discrete control-volume space using basic physical principles. This is also the first known application of a physically based monotonicity preserving transport scheme (flux-form semi-Lagrangian scheme) for modeling not only the scalars but also all the dynamical variables in a GCM. This new GCM features a physically inspired terrain following Lagrangian control-volume vertical coordinate.

The monotonicity preserving nature of this model is particularly advantageous for use in a data assimilation system. This is because the monotonic transport scheme can handle

strong gradients induced by the internal dynamics or the data insertion procedure better than any other schemes currently in use, e.g., the center differencing scheme or the spectral method. Another important feature of the finite-volume dynamical core is that it is free of the usual problem in computing the pressure gradient force near steep mountains.

Lin, S.-J., and R. B. Rood, Multidimensional Flux-form Semi-Lagrangian Transport Schemes, *Mon. Wea. Rev.*, 124, 2046-2070, 1996.

Lin, S.-J., and R. B. Rood, an Explicit Flux-form Semi-Lagrangian Shallow Water Model on the Sphere, *Quart. J. Roy. Met. Soc.*, 1997.

Lin, S.-J., A Finite-volume Integration Method for Computing Pressure Gradient Forces in General Vertical Coordinates, *Quart. J. Roy. Met. Soc.*, 1997.

Land Surface and Soil Hydrology Parameterization

Recent work with the land surface and soil hydrology parameterization known as the Parameterization for Land-Atmosphere-Cloud Exchange (PLACE) has confirmed on the continental scale what PLACE model results were first to show in 1987 on the local scale: that sub-resolvable heterogeneity of land surface characteristics can have a powerful effect on surface water and energy budgets.

Specifically, PLACE stand-alone runs made in conjunction with the Global Energy and Water-cycle Experiment (GEWEX)-sponsored international intercomparison (known as the Global Soil Wetness Project [GSWP]) demonstrated that spatial heterogeneity, particularly of soil properties, can strongly affect the grid-averaged and regional-basin-averaged model runoff. Careful treatment of this heterogeneity is, therefore, required.

In other studies, simulations with the PLACE model coupled with the Goddard Cumulus Ensemble model (GCE) evaluated the impact of dry/wet soil moisture patches and atmospheric boundary conditions on the formation and evolution of moist convection; there was a significant, systematic impact of soil patch size and background wind on moist convection, including cloud structure and rainfall. These results suggest the importance of landscape discontinuities on the generation of deep moist convection.

New parameterizations can be developed based on explicit cloud-resolving runs such as these, which parameterize the underlying mesoscale circulations generated by the landscape heterogeneity. Moreover, because of the transient, interactive nature of soil moisture with the precipitating clouds, these parameterizations need to account for the time-dependent nature of the patches themselves.

Lynn, B.H., W.-K. Tao, and P.J. Wetzell, A Study of Landscape-Generated Deep Moist Convection, *Mon. Wea. Rev.* (in press, 1997).

The Use of the Goddard Cumulus Ensemble Model in the Study of Regional Climate

The representation of clouds and precipitation in Cloud Resolving Models (CRMs) is arguably superior to GCMs and climate models, because CRMs solve the primitive equations with much greater spatial and temporal resolution using more sophisticated and physically realistic parameterizations of cloud microphysical processes. The CRM does not need a cumulus parameterization scheme, and it can allow explicit cloud-radiation interaction--cloud optical thickness is directly determined by hydrometeor amount, phase and size distribution. In CRM-climate studies, the CRM is typically run for several weeks, until modeled temperature and water vapor fields reach a statistical equilibrium state. However, numerical experiments from two different CRMs (the Goddard Cumulus Ensemble Model and the NCAR CRM), produced quite different statistical equilibrium states (cold/dry vs. warm/humid) even though both models contained cloud-radiation interactive processes and sea surface fluxes under very similar large-scale influences. Long term CRM (GCE model) sensitivity tests were performed to identify the "physical processes" that determine these two different statistical equilibrium states (or climates).

Both regimes (warm/moist and cool/dry) are simulated, are physically consistent, and have been predicted by simple atmosphere-ocean climate models. The major difference between runs that produced warm/humid and cold/dry climates is whether or not the convective processes are allowed to mix the horizontal wind, i.e., the role of convective momentum transport, which is a process not well understood in large-scale terms, and not represented in large-scale models. The simulated surface wind in runs that allowed convective mixing processes in horizontal momentum is only about 1 to 3 m/s, as compared with 10 m/s in runs without convective mixing. The runs that had stronger surface wind (and consequently larger latent and sensible heat fluxes from the ocean) produced a warmer and more humid modeled thermodynamic equilibrium state.

Our results also indicated that microphysics and its interaction with radiation as well as the diurnal cycle can not alter the model simulated equilibrium state from one regime (warm/humid) to another (cold/dry), but it can change the degree of the equilibrium state (i.e., from warm to warmer).

Tao, W.-K., J. Simpson, C.-H. Sui, C.-L. Shie, B. Zhou, K. M. Lau, M. Moncrieff, On Equilibrium (Climate) States Simulated by Cloud-resolving models, *Bull. Amer. Meteor. Soc.* (submitted, 1997).

Mission Support

Ozone Forecasts for POLARIS

During the Photochemistry of Ozone Loss in the Arctic Region in Summer (POLARIS) deployments of 1997, the Atmospheric Chemistry and Dynamics Branch used its three-dimensional chemistry and transport models to generate global five-day ozone forecasts. The objective was to provide a product which had the potential to aid flight planning. The forecasts utilized winds and temperatures from the DAO on a daily basis, and the processing stream produced northern hemisphere maps of forecast total ozone and ozone near ER-2 flight altitudes in the lower stratosphere. These maps were posted on the DAO's home page.

Producing the forecasts required both full and parameterized chemistry and transport models (CTMs). First, the full CTM was initialized with UARS Microwave Limb Sounder ozone data on 20 Mar, 1997, prior to the first deployment. Then, as each day's winds analysis became available, the full CTM was integrated through that respective 24-hour period. Second, the parameterized CTM used the full CTM's terminal ozone field as an initial condition and employed the DAO's forecast winds to simulate ozone during the coming five days.

In post-mission analysis, we are concentrating on the anomaly correlations between the forecast total ozone and that which is observed by ADEOS-TOMS and Earth Probe-TOMS. Note, however, that ozone is not assimilated in this process. The parameterized CTM used only a simplified ozone photochemistry, which allowed a five-day forecast to be produced in less than an hour.

The DAO produces real-time assimilation and forecast products in support of NASA stratospheric aircraft campaigns, Shuttle-borne stratospheric sounders, and space-based remote sensing platforms. GEOS DAS utilizes global meteorological observations collected by the National Center for Environmental Prediction (NCEP) and made available to the DAO via the GSFC DAAC. With the GEOS DAS, the DAO produces daily assimilated fields of meteorological variables and short-range forecasts. These global products are on a 2 degree latitude by 2.5 degree longitude grid, and extend from the Earth's surface to the upper stratosphere.

Douglass, A. R., C. J. Weaver, R. B. Rood, L. Coy, A Three-Dimensional Simulation Of The Ozone Annual Cycle Using Winds From A Data Assimilation System, *J. Geophys. Res.*, 101, 1463-1474, 1996

Nielson, J.E., , A.R. Douglass, R.B. Rood, S.D. Steenrod, M.c. Cerniglia, Total Ozone Anomaly Correlations in Forecasts for POLARIS Deployment 1, *Paper A21A-07, Fall AGU Meeting*, 1997

Real-Time Mission Support

The DAO provides real-time support to many NASA aircraft and space-based Earth observation missions.

The DAO provided operational data products to the Stratospheric Tracers of Atmospheric Transport (STRAT) aircraft campaign which ran from May 1995 through December 1996. This campaign involved six deployments out of NASA Ames Research Center in California and Barber's Point in Hawaii.

The DAO supported the Photochemistry of Ozone Loss in the Arctic Region in Summer (POLARIS) aircraft campaign, which started in April 1997 and which finished in September 1997. POLARIS had three deployments, primarily out of Ft. Wainwright in Fairbanks, Alaska. The final deployment ended with flights out of Barber's Point in Hawaii.

GSFC Atmospheric Chemistry and Dynamics Branch (ACDB) researchers in the field used the forecast products for scientific flight planning, where they asked the ER-2 pilot to take measurements along a certain track or in a certain region based on the GEOS DAS forecast. Additionally, an archive of assimilated dynamical quantities from the GEOS DAS provides background information for interpretation of the constituent data measured by the ER-2.

The second Cryogenic Infrared Spectrometers and Telescopes for the Atmosphere (CRISTA) experiment, which flew on STS-85 (Discovery) in August 1997, received support from the DAO as well. The DAO provided assimilated fields and forecasts of temperature and potential vorticity from each day's GEOS DAS run to the CRISTA science team.

The DAO is now providing one of the input data sources needed to produce retrievals from the Clouds and the Earth's Radiant Energy System (CERES) instrument, scheduled for launch aboard the TRMM satellite in late 1997. The DAO began sending GEOS DAS assimilation products to CERES via the NASA Langley Research Center Distributed Active Archive Center (DAAC) in August 1997. These data sets include surface, boundary layer, and upper air variables. The CERES team will test their processing software using DAO fields. DAO support to CERES after TRMM launch will be accomplished in a similar manner, but will be performed using a new release of the GEOS DAS.

Research from Geostationary Platforms

Advanced Geostationary Studies (AGS)

In 1997, NASA's Earth Science Enterprise requested that GSFC propose Advanced Geosynchronous Studies (AGS) for components of mutual interest to NOAA and NASA. A joint NASA-NOAA group was formed to take part in these studies. The project scientist for the AGS comes from the Laboratory. The AGS is managed by the Systems Technology and Advanced Concepts Directorate (STAAC).

During 1998, AGS will foster advanced geosynchronous instruments for the next GOES satellite system in order to meet the projected forecast requirements from the National Weather Service (NWS), complement the remote sensing requirements of Earth Science and the United States Global Change Research Program (USGCRP), and infuse into various missions potent hardware now being made available by the defense industry. There is general agreement for advancement in NOAA's GOES weather satellite instruments in the next decade to complement the EOS observations for monitoring short-term climate. These instrument include:

- A fast multi-spectral imager, with 2 km or better resolution in all atmospheric windows, a SNR>500:1, and four or more full-disk images per hour;
- A high-resolution infrared sounder, with hourly full-disk scans at 10 km resolution and spectral resolution>2000:1;
- A microwave sounder, with hourly coverage at 20 km or better resolution in temperature and moisture lines;
- A lightning mapper, with minute-by-minute coverage at 10 km resolution; and
- An automated ground system, with standard data bases and real-time data distribution.

Space Flight Missions

Cassini Mission to Saturn

The Cassini Mission to Saturn is a joint effort between NASA and the European Space Agency (ESA). The Cassini Mission is managed for NASA by the Jet Propulsion Laboratory (JPL) in Pasadena, California, where the Cassini orbiter was designed and assembled. A team based at ESA's European Space Technology and Research Center (ESTEC) in Noordwijk, the Netherlands, managed development of the Huygens Probe, destined to take measurements of Titan's atmosphere. The Atmospheric Experiment Branch delivered two instruments, the Ion and Neutral Mass Spectrometer (INMS) for the Orbiter, and the Gas Chromatograph-Mass Spectrometer (GCMS) for the Huygens Probe.

The GCMS is a very versatile gas chemical analyzer designed to identify and quantify the abundances of various constituents in the atmosphere of Titan, including argon, other noble gases, and isotopes. The flight model (FM) and the flight spare (FS) were delivered in 1997 for integration on the Huygens Probe.

The INMS is intended to measure the positive ion and neutral species composition and structure in the upper atmosphere of Titan, and the ion and neutral environments of Saturn's icy satellites, rings and magnetosphere. The INMS engineering model (EM) and the flight model (FM) were delivered to the JPL for integration on the Saturn Orbiter.

The Cassini Spacecraft was launched October 15, 1997 with Saturn encounter in 2004.

Analysis of the Jovian Atmosphere

The Atmospheric Experiment Branch's contribution to the Galileo mission to Jupiter was the mass spectrometer on the Galileo Probe. Shortly before arrival at Jupiter in December 1995, the Probe separated from the Galileo Orbiter, entered the atmosphere, and descended on a parachute into the deep Jovian atmosphere. Data were collected by the mass spectrometer for 57 minutes, at atmospheric pressures ranging from approximately 0.3 to 23 times Earth sea level pressure, at which point Probe data transmission stopped. Analysis of the data has continued through 1997.

The Galileo Probe Mass Spectrometer (GPMS) was the primary Probe instrument to measure chemical composition of the atmosphere of Jupiter, which consists primarily of hydrogen and helium, with smaller amounts of water, methane, ammonia, hydrogen sulfide, and lower concentrations of other molecules. The Galileo Probe Mass Spectrometer measured variations in the abundance of all these species as a function of altitude and detected other species in the atmosphere such as the chemically inert noble gases as shown in Figure 12. A comparison of noble gas abundances on other planets and the Sun will help distinguish between possible mechanisms of planetary formation and evolution of planetary atmospheres. Since Jupiter is the most massive planet in the solar system, the noble gas abundances found there are expected to closely reflect the abundances in the solar nebula from which the planets formed.

Galileo Probe Entry Into the Atmosphere of Jupiter December 7, 1995

GPMS spectra in the 17 to 18.5 bar region of Jupiter's atmosphere

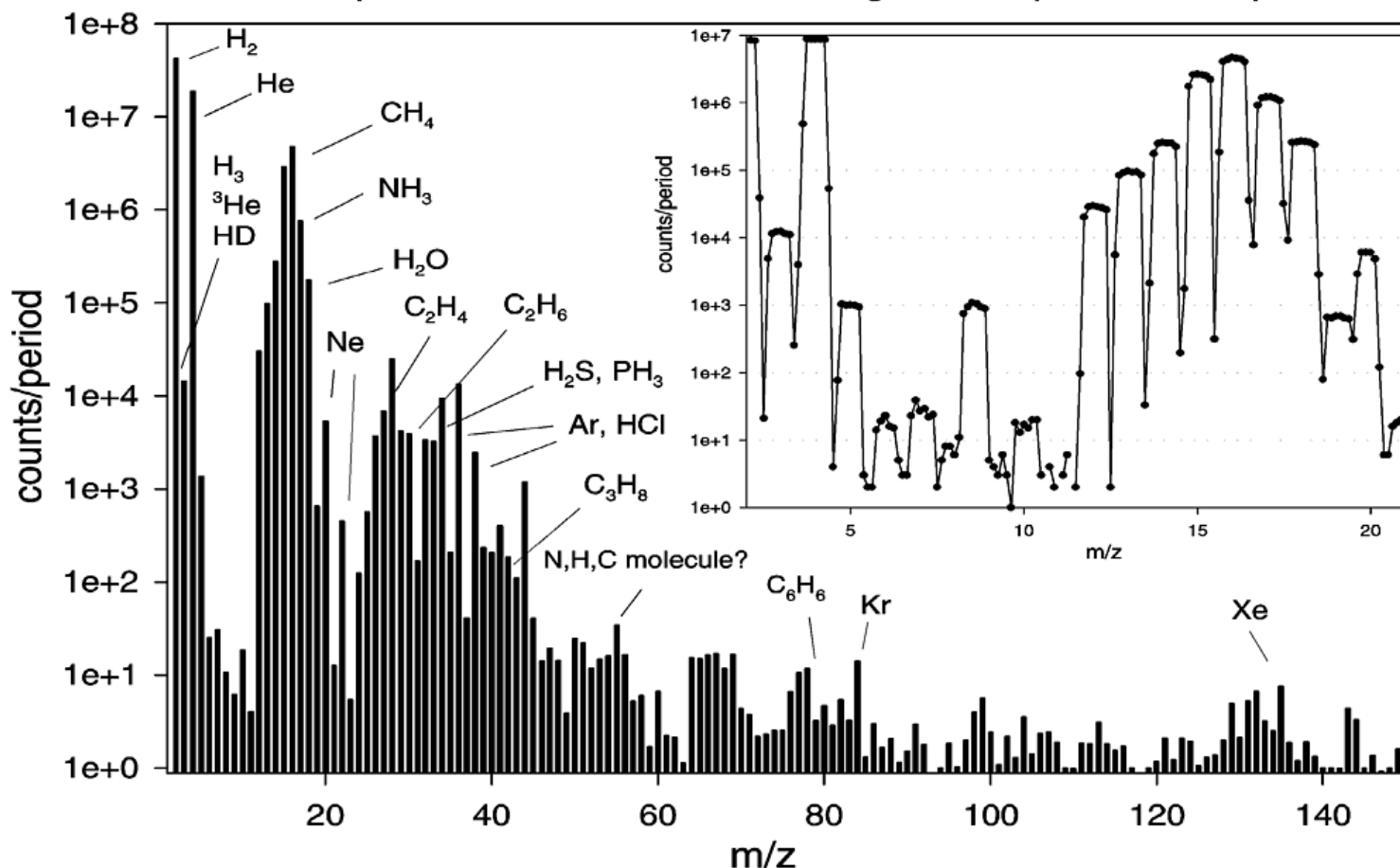


Figure 12

Atmospheric species with molecular weights from 2 to 150 Atomic Mass Units were analyzed, and signals from more than 6000 values of mass-to-charge ratios were taken during the descent. Preliminary findings indicate that the abundance ratio of helium to hydrogen in the atmosphere is near but slightly lower than the solar value at 0.156 (by volume), while the abundance ratio of methane is higher. The abundance ratio of water during the early part of the descent is surprisingly lower than those predicted using solar values of carbon and oxygen (i.e., a much dryer atmosphere was found than was expected). However, hydrogen sulfide, water, and other condensable species show a substantial increase in mixing ratio at the highest pressures encountered during the descent. These observations, coupled with the observation that the Probe entered Jupiter in a relatively cloud-free region and in an infrared hot spot, are presently stimulating a reevaluation of prior models and enabling a new understanding of the atmospheric circulation on Jupiter.

Atreya, S., M. Wong, T. Owen, H. Niemann, and P. Mahaffy, Chemistry and Clouds of the Atmosphere of Jupiter. A Galileo Perspective, in *Three Galileos: The Man, The Spacecraft, The Telescope*, J. Rache, C. Barbieri, T. Johnson, A. Sohus, Eds., Kluwer Academic Publishers, Dordrecht, 1997

Tropical Rainfall Measuring Mission (TRMM)

NASA's Tropical Rainfall Measuring Mission (TRMM) was successfully launched from Tanegashima space complex in Japan on November 27, 1997. The TRMM mission is the first international Earth science mission dedicated to measuring tropical and subtropical rainfall through microwave and visible/infrared sensors. It includes the first spaceborne radar, supplied by the Communications Research Laboratory of Japan. The spacecraft was built and integrated within Goddard's Space Flight Center's Projects Directorate. TRMM will permit documentation of the vertical profile of rain, which is related to the vertical profile of latent heat release. TRMM's orbit will precess through the diurnal cycle, giving the first look at the diurnal cycle of tropical precipitation on a global scale.

Much of the Laboratory activity has centered around developing and testing algorithms needed to retrieve rainfall and the latent heating from current sensors and cloud scale cumulus models. Recent results indicate that passive microwave observations can be used to delineate convective from stratiform rain and to derive estimates of the latent heating profile. These results will allow TRMM observations to be utilized to study not only the impact of the heating on the global climate, but also the heating distributions related to convective systems and cyclonic storms, including hurricanes. The TRMM observations will also be used to calibrate precipitation estimates based on data from other satellites (including polar orbiting and geosynchronous) and rain gauge networks to produce merged surface precipitation estimates of higher quality than previously available. Ground validation activities are supported by the TRMM office in the Laboratory.

Hong, Y., C. Kummerow, and W. S. Olson, Separation of Convective/Stratiform Precipitation using Microwave Brightness Temperatures., *J. Applied Meteorology*, (submitted, 1997)

Huffman, G. J., R.F. Adler, P. Arkin, A. Chang, R. Ferraro, A. Gruber, J. Janowiak, A. McNab, B. Rudolf, U. Schneider, The Global Precipitation Climatology Project (GPCP) Combined Precipitation Data Set, *Bull. Am. Meteor. Soc.*, 78, 5-20, 1997

Infrared Spectral Imaging Radiometer on STS-85

The Infrared Spectral Imaging Radiometer (ISIR) is a Space Shuttle Hitchhiker instrument flown on the twelve-day STS-85 mission in August 1997. ISIR was designed and developed in cooperation with industry and Department of Energy (DOE) partners to apply new techniques and technology for cloud observations from space. Specifically, the scientific mission of ISIR is to provide radiometrically calibrated cloud top imagery, and to obtain information on the distribution of infrared radiation parameters and particle size of high altitude clouds.

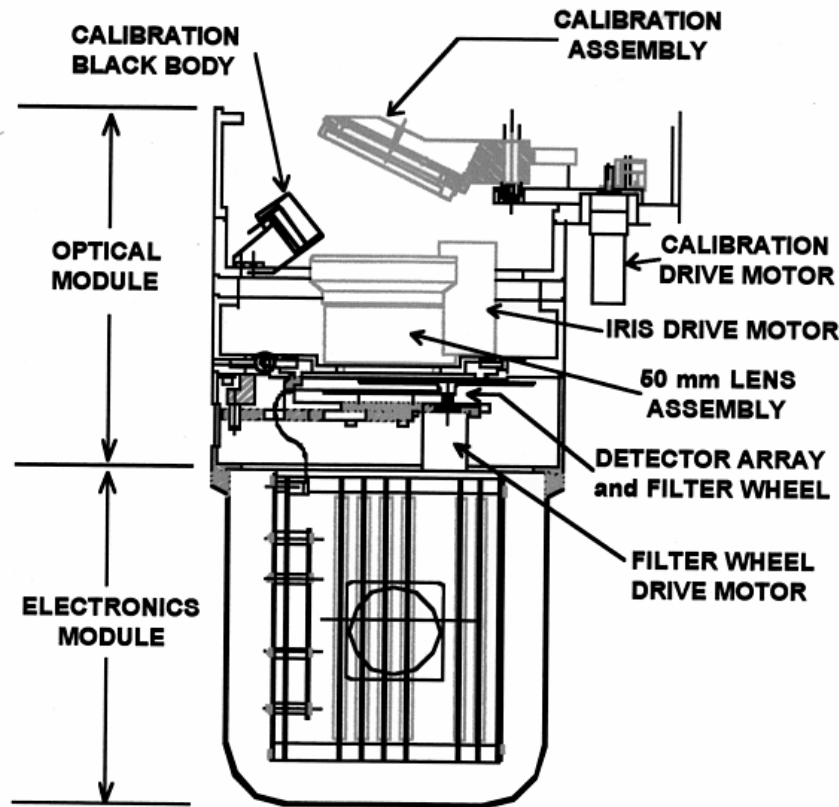


Figure 13. Schematic diagram of the Infrared Spectral Imaging Radiometer.

ISIR is a multispectral imaging radiometer. It measures infrared radiation emitted from cloud tops in three narrow spectral bands centered at 8.6, 11.0, and 12.0 microns, and in a broad band from 7 to 13 microns. An advanced technology detector with the potential to greatly reduce the size and cost of cloud imagers was tested in the instrument. An uncooled microbolometer array (MBA) detector with 80,000 pixels at the focal plane of the instrument senses infrared radiation and provides spectral imagery with a resolution of 250 m. Resolution at this level is thought to be optimal for accurate cloud coverage detection in general. The STS-85 global data set of spectral infrared images at 250 m resolution is a unique resource for atmospheric science that has direct utility to address the science priorities of NASA's Earth Science Enterprise and the problems of global climate change.

Initial analysis of the data has shown some dramatic results. Many aircraft contrails are seen in data from northern Canada and Europe. One current research interest involves the potential effects of aviation on climate, and in particular the effects of contrails. The one kilometer or lower resolution of existing satellite thermal infrared imagery is not adequate to detect all contrails. Improved contrail detection from the higher 250 m resolution of ISIR was a significant goal of the experiment.

The ISIR Shuttle flight was done in coordination with the Shuttle Laser Altimeter (SLA). The laser altimeter instrument gives direct measurements of cloud heights. For the first time, the combination of ISIR and SLA will allow cloud observation techniques based on the combination of passive infrared and active laser sensing to be applied from space. A reflight of ISIR and SLA is planned for late 1998.

Spinhirne, J.D., W.D. Hart, D.P. Duda, Evolution of the Morphology and Microphysics of Contrail Cirrus from Airborne Active and Passive Remote Sensing, *Geoph. Res. Let.*, 23 (submitted, 1997).

[Back to Table of Contents](#)
[Forward to Section 7](#)

[Send e-mail](#) to the maintainer of this page.
 The responsible NASA official is [Bob Theis](#).